

# Generic Contrast Agents

Our portfolio is growing to serve you better. Now you have a *choice*.



[VIEW CATALOG](#)

# AJNR

This information is current as of May 25, 2025.

## **Clinical and Imaging Findings in Children with Myelin Oligodendrocyte Glycoprotein Antibody Associated Disease (MOGAD): From Presentation to Relapse**








Elizabeth George, Jeffrey B. Russ, Alexandria Validighi, Heather Early, Mark D. Mamlouk, Orit A. Glenn, Carla M. Francisco, Emmanuelle Waubant, Camilla Lindan and Yi Li

*AJNR Am J Neuroradiol* 2024, 45 (2) 229-235

doi: <https://doi.org/10.3174/ajnr.A8089>

<http://www.ajnr.org/content/45/2/229>

# Clinical and Imaging Findings in Children with Myelin Oligodendrocyte Glycoprotein Antibody Associated Disease (MOGAD): From Presentation to Relapse

 Elizabeth George,  Jeffrey B. Russ,  Alexandria Validighi, Heather Early,  Mark D. Mamlouk,  Orit A. Glenn,  Carla M. Francisco, Emmanuelle Waubant,  Camilla Lindan, and  Yi Li



## ABSTRACT

**BACKGROUND AND PURPOSE:** Myelin oligodendrocyte glycoprotein-antibody associated disease (MOGAD) is an increasingly recognized cause of demyelinating disease in children. The purpose of this study is to characterize the CNS imaging manifestations of pediatric MOGAD and identify clinical and imaging variables associated with relapse.

**MATERIALS AND METHODS:** We retrospectively identified children with serum antibody-positive MOGAD evaluated at our institution between 1997 and 2020. Clinical and demographic data were collected. MRIs of the brain, orbit, and spine at presentation and relapse were reviewed for location and pattern of abnormality.

**RESULTS:** Among 61 cases (34 girls), mean age at presentation was 7 years (IQR 4–11). At presentation, there was imaging involvement of the brain in 78.6% (44/56), optic pathway in 55.4% (31/56), and spine in 19.6% (11/56). Brain involvement was commonly in the frontal (70.5%, 31/44) and subcortical (75%, 33/44) white matter, with involvement of the thalamus and pons in 47.7% each (21/44). Optic neuritis (ON) was commonly bilateral (80.6%, 25/31) involving intraorbital segments (77.4%, 24/31). Spinal cord lesions were typically cervical (72.7%, 8/11) and multifocal (72.7%, 8/11).

The imaging patterns were age-dependent; children  $\leq 9$  years more commonly demonstrated ADEM-like imaging pattern at presentation (39.4%, 13/33) and first relapse (8/23, 34.8%), while children  $> 9$  years more commonly had ON at presentation (34.8%, 8/23,  $P = .001$ ) and FLAIR-hyperintense lesions in anti-MOG-associated encephalitis with seizures at first relapse (5/18, 27.8%,  $P = .008$ ).

**CONCLUSIONS:** We describe the CNS imaging findings in pediatric MOGAD. The imaging pattern is age-dependent at presentation and first relapse. Younger age at presentation is associated with longer time to relapse.

**ABBREVIATIONS:** ADEM = acute disseminated encephalomyelitis; DGN = deep gray nuclei; FLAMES = FLAIR-hyperintense lesions in anti-MOG-associated encephalitis with seizures; MOG = myelin oligodendrocyte glycoprotein; MOGAD = MOG-antibody associated disease; NMOSD = neuromyelitis optica spectrum disorder; ON = optic neuritis

Since myelin oligodendrocyte glycoprotein (MOG) was identified as a target antigen in acute disseminated encephalomyelitis (ADEM),<sup>1</sup> MOG-antibody associated disease (MOGAD) is increasingly recognized as a major cause of demyelinating disease in children and adults.<sup>2–4</sup> MOGAD has a distinct clinical course and management<sup>5,6</sup>

compared with other demyelinating diseases, such as multiple sclerosis and neuromyelitis spectrum disorders (NMOSD), and the ability to prospectively suspect MOGAD based on initial clinical manifestations and imaging phenotype<sup>7,8</sup> would allow for targeted antibody testing and prompt treatment.

While MOGAD has an overall better clinical course compared with NMOSD, a certain proportion of patients will develop relapsing disease (28%–62%)<sup>4,7,9–11</sup> with long-term neurologic sequelae.<sup>12</sup>

Additionally, pediatric patients manifest differently compared with adult patients,<sup>13</sup> and the spectrum of MOGAD is still being defined in the pediatric population, with only a few prior small studies<sup>11,13–17</sup> and recently proposed diagnostic criteria.<sup>18</sup> There is currently limited imaging description at the time of diagnosis and relapse.

The purpose of this study is to comprehensively characterize the brain, orbit, and spine imaging manifestations of pediatric

Received June 29, 2023; accepted after revision November 7.

From the Departments of Radiology and Biomedical Imaging (E.G., O.A.G., C.L., Y.L.), and Neurology (C.M.F., E.W.), Division of Child Neurology (A.V.), University of California San Francisco, San Francisco, California; Department of Pediatrics (J.B.R.), Division of Neurology, Duke University, Durham, North Carolina; Department of Radiology (H.E.), University of Texas Southwestern, Dallas, Texas; and Permanente Medical Group (M.D.M.), Kaiser Permanente Medical Center Santa Clara, Santa Clara, California.

Please address correspondence to Elizabeth George, MBBS, Department of Radiology and Biomedical Imaging, University of California San Francisco, 505 Parnassus Ave, San Francisco, CA 94143; e-mail: Elizabeth.george@ucsf.edu; @LizzRad

 Indicates article with online supplemental data.

<http://dx.doi.org/10.3174/ajnr.A8089>

MOGAD at presentation and relapse in a large institutional cohort of seropositive MOGAD, and to identify clinical and imaging variables associated with a relapsing phenotype.

## MATERIALS AND METHODS

Patients were identified retrospectively from the University of California San Francisco pediatric neuroimmunology clinic database, which includes all patients seen between 1997 and 2020. Patients were eligible for inclusion if they had clinical evidence of a noninfectious neuroinflammatory syndrome, at least 1 serologic anti-MOG titer of 1:20 or greater by using a cell-based assay (Mayo Clinic) either while acutely symptomatic or on a banked study serum sample (particularly for patients included in the cohort before routine anti-MOG antibody testing), had clinical exclusion of reasonable alternative diagnoses, and MR imaging available at presentation or at any of the first 2 relapses (Online Supplemental Data). This study was conducted with approval by the Institutional Review Board and in compliance with all policies on the responsible conduct of human research. The need for informed consent was waived. Some of the clinical and CSF analysis of this cohort has been reported previously.<sup>19</sup>

### Clinical and Laboratory Data

Clinical data were collected via retrospective chart review and included clinical features that were documented by a pediatric neurologist who either directly cared for the patient during the initial presentation or who subsequently followed the patient on an outpatient basis. In nearly all cases, relapse was defined as a distinct recurrence of symptomatology following a period of symptom resolution for an interval of at least 2 weeks, which was also confirmed radiographically. In a minority of cases, episodes were still felt to qualify as clinical relapse if based on high clinical suspicion by a trained neuroimmunologist or pediatric neurologist, even in the absence of radiographic confirmation. We collected clinical data from the initial presentation and up to 2 relapses, including age, time to relapse, clinical symptoms, and serum anti-MOG and anti-AQP4 titers either at presentation or on a banked specimen. MOG-IgG testing with a cell-based assay (Mayo Clinic) was done on clinical samples after 2017 when the test became commercially available and on banked research samples for samples collected before 2017. The total number of clinical relapses, up to 10, and total length of follow-up were documented.

### Imaging

All clinical MRIs of the brain, orbit, and spine within 3 months of initial presentation and relapse available in our institutional PACS were reviewed, including those performed at outside institutions.

The MRIs were reviewed by 3 pediatric neuroradiologists with 7–32 years' experience. At the initiation of the study, 10 randomly selected MRIs were reviewed by all reviewers separately and then together by consensus to achieve consistency in scoring. Interreader reliability was assessed on overall imaging pattern in these 10 cases. Given strong interreader reliability (see Results), each subsequent study was reviewed by 1 reviewer and reviewers met periodically thereafter to maintain uniformity in scoring. Detailed imaging review included the assessment of location, symmetry, size, and characterization of abnormalities of the brain,

optic nerves, and the spine (Online Supplemental Data). Locations of involvement were chosen based on prior descriptions in the literature.<sup>15,17,20</sup> Supratentorial locations were characterized as cortex, deep gray nuclei (DGN; caudate, putamen, globus pallidus, thalamus), and white matter (subcortical, deep, periventricular, internal capsule, corpus callosum). The white matter involvement was classified based on lobes involved (frontal, parietal, temporal, and occipital lobes and the insula). The infratentorial regions involved were categorized as midbrain, pons, medulla, brachium pontis, cerebellum, or other. The parenchymal involvement was assessed for size (small, intermediate, or large; Online Supplemental Data). Noncortical involvement was assessed for margin characteristics (well-defined, ill-defined, or mixed) and degree of confluence (discrete, beginning confluence, or confluent). Other imaging features assessed were presence and pattern of enhancement (cortical, leptomeningeal, solid/nodular, peripheral ring, or incomplete ring), presence of reduced diffusion on DWI, and abnormal susceptibility on SWI/gradient echo. Orbital images were evaluated for unilateral versus bilateral involvement, segments of optic nerve abnormality, optic nerve enhancement, perineural enhancement, and presence of reduced diffusion. When dedicated orbital imaging was not available, the orbits were assessed on whole-brain sequences if deemed to be of sufficient quality by the reviewers. Spine involvement was characterized as long (spanning  $\geq 3$  vertebral bodies) or short segment (spanning  $< 3$  vertebral bodies), unifocal or multifocal, region of involvement (cervical, thoracic, conus, or cauda equina), cross-sectional pattern (central, peripheral, holocord, or gray matter only), presence of cord expansion, and pattern of enhancement (none, intramedullary, or leptomeningeal). When spine DWI was available, the presence of reduced diffusion was assessed.

The overall imaging pattern was characterized as ADEM-like, optic neuritis (ON), myelitis (any cord signal abnormality), FLAIR-hyperintense lesions in anti-MOG-associated encephalitis with seizures (FLAMES), or any combination of the above. ADEM-like pattern was defined as multifocal supratentorial or infratentorial white or gray matter T2/T2-FLAIR hyperintense lesions with or without enhancement (Fig 1). When FLAMES occurred in combination with other patterns (ADEM-like, ON, or myelitis), the overall pattern was assigned as FLAMES (Fig 2).

### Statistical Analysis

Interreader reliability was assessed using the Cohen kappa coefficient. The association of age ( $\leq 9$  years versus  $> 9$  years established based on prior literature)<sup>5</sup> and anti-MOG titer with imaging pattern at presentation, presence of clinical relapse, and time to clinical relapse were assessed using the Student *t* test and Wilcoxon rank sum test, as appropriate. The association of imaging pattern with patient age and occurrence of relapse was assessed by using the Fischer exact test. The threshold for significance for all tests was set at  $P < .05$ . All statistical tests used Stata 14.0 (College Station, TX).

## RESULTS

Sixty-one patients were included in the study. The median age at presentation was 7 years (IQR: 4–11). The study population was 55.7% (34/61) female.

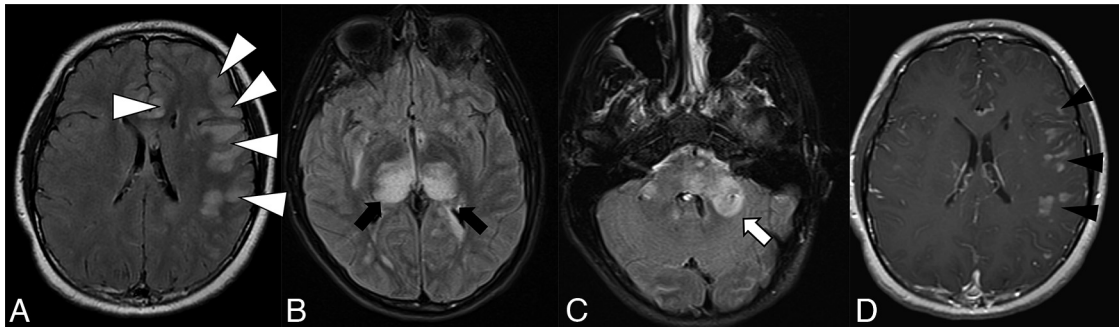


**FIG 1.** Thirteen-year-old adolescent boy who presented with encephalopathy after a viral prodrome, found to have papilledema and opening pressure >39, subsequently found to have serum positivity for anti-MOG antibody. Brain MR imaging demonstrates features of ADEM-like pattern of pediatric MOGAD. A-C, FLAIR hyperintensity involving the left frontal subcortical white matter with ill-defined borders and beginning confluence (white arrowheads), bilateral thalami (black arrows), pons and brachium pontis (white arrow). D, Solid nodular enhancement associated with the left frontal white matter lesions.

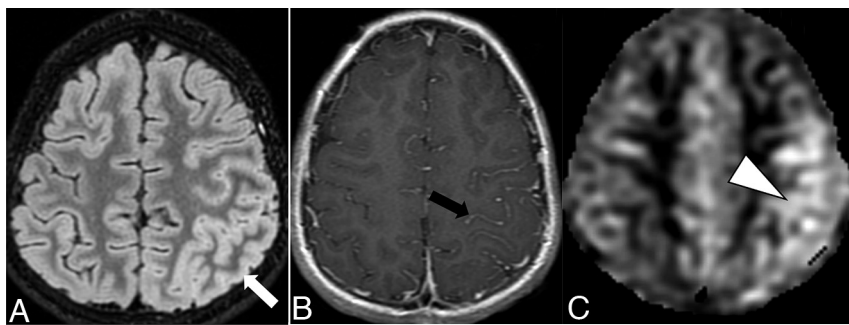


**FIG 2.** Ten-year-old boy with rapid-onset altered mental status and seizures. A, Cortical FLAIR hyperintensity (white arrow) involving the left parietal lobe. B, Associated leptomeningeal enhancement (black arrow). C, Concurrently acquired arterial spin labeling image demonstrates hyperperfusion of the left parietal cortex (white arrowhead), reflective of associated seizure activity.

156/239 (65.2%), 3T in 78/239 (32.6%), 1T in 3/239 (1.3%), and unknown in 2/239 (0.8%).

**Presentation.** MR imaging at presentation was available in 91.8% (56/61) of patients, including 56 brain, 18 orbit, and 29 spine MR images.

The imaging characteristics are summarized in Tables 2 and 3. At presentation, there was intracranial involvement in 78.6% (44/56), orbital in 55.4% (31/56), and spinal in 19.6% (11/56). Among those with intracranial abnormalities, the frontal lobe white matter was the most commonly involved (31/44, 70.5%), with the sub-

### Clinical Relapse

The median follow-up time was 6 years (IQR: 3–13 years). Of the study cohort, 73.7% (45/61) had at least 1 relapse and 52% (32/61) had at least 2 relapses. The median time to first relapse was 5 months (IQR: 2–13), and median time between first and second relapse was 8 months (IQR: 2–25.25). Age at presentation was not associated with the presence of relapse (8.7 years without relapse versus 7.8 years with relapse,  $P = .45$ ). The mean follow-up time was longer among those  $\leq 9$  years (10.1 years) compared with those  $> 9$  years (5.6 years,  $P = .003$ ). Older age ( $> 9$  years) at presentation was associated with shorter time to first relapse (4.6 versus 18.8 months,  $P = .04$ ).

### Clinical and Laboratory Data

The most common clinical syndrome at presentation was ON (50.8%, 31/61), followed by ADEM (23%, 14/61) and myelitis (19.7%, 12/61, Table 1). The baseline anti-MOG titer was not significantly different between those with and without relapse (1:100 versus 1:100,  $P = .84$ ). None of the cases had a positive anti-AQP4 titer.

### Imaging Findings

A total of 239 MRIs in 61 patients were reviewed, including 125 brain, 52 orbit, and 62 spine MRIs. MRIs were scanned at 1.5T in

cortical location being most common (33/44, 75%). The thalamus was the most commonly affected DGN (21/44, 47.8%), and the pons was most commonly affected infratentorial structure (21/44, 47.7%). The lesions commonly had ill-defined margins (32/42, 76.2%) and were beginning to demonstrate confluence (18/42, 42.9%). A range of enhancement patterns was noted, most commonly solid/nodular (17/44, 38.6%) or linear (10/44, 22.7%). The presence of reduced diffusion was rare (4.5%, 2/44), and no cases (0/36) had abnormal magnetic susceptibility.

Orbital involvement was more commonly bilateral (25/31, 80.6%) and more commonly involved the intraorbital segments of the optic nerve (24/31, 77.4%). Most cases with orbital involvement demonstrated optic nerve (86.2%, 25/29) and perineural (68%, 17/25) enhancement.

Spinal cord involvement was more commonly short segment (6/11, 54.5%), multifocal (8/11, 72.7%), with frequent involvement of the cervical cord (8/11, 72.7%). There was a spectrum of involvement of the cross-section of the cord (Table 3), and cord enhancement was uncommon (3/11, 27.3%).

The most common imaging pattern at presentation was ADEM-like (14/56, 25%), followed by ADEM-like with ON (13/56, 23.2%, Fig 3). There was strong interreader reliability in the assessment of overall imaging pattern ( $\kappa = 0.84$ ).



**Relapse.** MR imaging was available in 91.1% (41/45) of patients at the first relapse. MR imaging was available in 87.5% (28/32) of patients with a second relapse.

**Table 1: Demographics and clinical data at time of diagnosis in cohort of pediatric patients with MOGAD**

|   | <i>n</i> = 61       |
|---|---------------------|
| Age, median (IQR), years                    | 7 (4–11)            |
| Female (%)                                  | 34 (55.7)           |
| Race (%)                                    |                     |
| African American                            | 6 (9.8)             |
| Hispanic                                    | 13 (21.3)           |
| White                                       | 22 (36.1)           |
| Other                                       | 14 (23.0)           |
| Unknown                                     | 6 (9.8)             |
| Initial clinical presentation               |                     |
| Syndrome                                    |                     |
| ADEM  | 14 (23.0)           |
| ON  | 31 (50.8)           |
| Myelitis                                    | 12 (19.7)           |
| Symptom                                     |                     |
| Headache                                    | 19 (31.1)           |
| Altered mental status                       | 12 (19.7)           |
| Ataxia                                      | 7 (11.5)            |
| Fever                                       | 11 (18.0)           |
| Seizure                                     | 2 (3.3)             |
| Anti-MOG titer, median (IQR) <sup>a</sup>   | 1:100 (1:80–1:1000) |
| Relapsing disease                           | 45 (73.8)           |
| Total episodes up to 10, median (IQR)       | 3 (1–4)             |
| Time to first relapse, median (IQR), months | 5 (2–13)            |

<sup>a</sup>Titer while acutely symptomatic during initial presentation was not available for 45 patients.

**Table 2: Brain MR imaging features at presentation for serum antibody-positive MOGAD**

| Brain Involvement           | <i>n</i> = 44 |                               | <i>n</i> = 44 |
|-----------------------------|---------------|-------------------------------|---------------|
| Supratentorial              | 41/44 (93.2)  | Margins <sup>a</sup>          |               |
| Cortex                      | 9/44 (20.5)   | Well-defined                  | 3/42 (7.1)    |
| Deep gray <sup>b</sup>      | 26/44 (59.1)  | Ill-defined                   | 32/42 (76.2)  |
| Caudate                     | 9/44 (20.5)   | Mixed                         | 7/42 (16.7)   |
| Putamen                     | 9/44 (20.5)   | Confluence <sup>a</sup>       |               |
| Globus pallidus             | 6/44 (13.6)   | Discrete                      | 16/42 (38.1)  |
| Thalamus                    | 21/44 (47.7)  | Beginning confluence          | 18/42 (42.9)  |
| White matter <sup>b</sup>   |               | Confluent                     | 8/42 (19)     |
| Frontal lobe                | 31/44 (70.5)  | Mass effect                   | 19/44 (43.2)  |
| Parietal lobe               | 28/44 (63.6)  | Enhancement <sup>b</sup>      |               |
| Temporal lobe               | 22/44 (50)    | Solid/nodular                 | 17/44 (38.6)  |
| Occipital lobe              | 19/44 (43.2)  | Peripheral ring               | 0             |
| Insula                      | 21/44 (47.7)  | Incomplete ring               | 1/44 (2.3)    |
| White matter <sup>b</sup>   |               | Ill-defined                   | 9/44 (20.5)   |
| Subcortical                 | 33/44 (75)    | Linear                        | 10/44 (22.7)  |
| Deep                        | 17/44 (38.6)  | Leptomeningeal                | 4/44 (9.1)    |
| Periventricular             | 14/44 (31.8)  | Cortical                      | 0/44          |
| Internal capsule            | 9/44 (20.5)   | None                          | 17/44 (2.3)   |
| Corpus callosum             | 8/44 (18.2)   | >1 enhancement characteristic | 10/44 (22.7)  |
| Infratentorial <sup>b</sup> | 31/44 (70.5)  | Low diffusivity <sup>c</sup>  | 2/43 (4.7)    |
| Midbrain                    | 15/44 (34.1)  | Susceptibility <sup>d</sup>   | 0/36          |
| Pons                        | 21/44 (47.7)  |                               |               |
| Medulla                     | 9/44 (20.5)   |                               |               |
| Brachium pontis             | 12/44 (27.3)  |                               |               |
| Cerebellum                  | 15/44 (34.1)  |                               |               |
| Other                       | 5/44 (11.4)   |                               |               |

<sup>a</sup>Not applicable in 2 cases of cortical only involvement.

<sup>b</sup>Percentages do not add up to 100% as many cases had multiple combinations of features.

<sup>c</sup>Unknown in 1 patient due to lack of DWI sequence.

<sup>d</sup>Unknown in 8 patients due to lack of SWI/gradiant echo sequence.

The imaging patterns were significantly different at relapse time points, with the combination of ADEM-like and ON (10/41, 24.4%) being the most common pattern at first relapse, and ADEM-like alone (11/29, 37.9%) being the most common pattern at second relapse ( $P = .01$ , Fig 3; Online Supplemental Data). There was a change in imaging pattern between presentation and first relapse in 69.4% (25/36) and between first and second relapse in 65.3% (17/26).

### Association of Clinical Variables and Imaging Findings

At presentation, ADEM-like (13/33, 39.4%) was the most common imaging pattern in younger children (age  $\leq 9$  years) whereas ON (8/23, 34.8%) was most common in older children ( $> 9$  years of age,  $P = .001$ , Table 4). At first relapse, the imaging pattern also differed by age ( $P = .008$ ); ADEM-like (8/23, 34.8%) was most common among those  $\leq 9$  years, while FLAMES (5/18, 27.8%) was most common in older children at first relapse. The imaging patterns were not significantly associated with age at second relapse ( $P = .21$ ). The imaging pattern at presentation was not significantly associated with occurrence of future relapse ( $P = .24$ ).

### DISCUSSION

Our study provides detailed characterization of imaging patterns of CNS involvement in a large cohort of children with MOGAD. We demonstrate an age-dependent imaging phenotype, which persists into first relapse. Furthermore, we demonstrate that imaging phenotypes often differ at relapse compared with presentation. Older age at presentation is associated with shorter time to relapse.

MOGAD is increasingly recognized as a major cause (21%–75%) of pediatric acquired demyelinating disease.<sup>2–4</sup> Proposed diagnostic criteria<sup>18</sup> and spectrum of imaging manifestations of MOGAD are being defined. Much of the previous literature on imaging manifestations of MOGAD include pediatric and adult populations<sup>8,21–23</sup> and do not provide systematic, detailed radiologic descriptions. In our detailed radiologic study of pediatric MOGAD, lesions at presentation involved predominantly the frontal subcortical white matter and DGN in the supratentorial brain and pons in the infratentorial brain. The lesions were often ill-defined and beginning to confluence, with solid/nodular enhancement, but without reduced diffusion or magnetic susceptibility. This is in agreement with limited previous studies with 10–69 patients which demonstrate predominantly poorly demarcated brain lesions involving the subcortical white matter and DGN in pediatric MOGAD.<sup>11,13–17</sup> The involvement of subcortical white matter as well as pontine involvement is a distinction from NMOSD, which

more commonly affects periventricular white matter and area postrema,<sup>24</sup> in addition to the presence of T1 hypointensity and lack of cortical involvement in NMOSD.<sup>14</sup> MOGAD lesions rarely involve the corpus callosum and are distinct from the small well-defined lesions seen in MS.<sup>10,11,14</sup> Incomplete ring pattern of enhancement, characteristic of MS, was seen in only 1 subject in our study. No cases in our cohort had signal abnormality on SWI;

thus, the presence of SWI abnormality suggests an alternative diagnosis.

Similar to prior studies, optic nerve involvement in our study was commonly bilateral and displayed anterior predominance compared with posterior predominance in NMOSD,<sup>13</sup> with a high prevalence of perineural enhancement (68%) similar to previous reports of 41%–52%.<sup>25,26</sup>

Reports of spine involvement in MOGAD are variable. Many of our cases had short segment, multifocal spinal cord involvement, with the cervical cord most affected. While initial reports of MOGAD favored a lower cord/conus predominance,<sup>20,27,28</sup> later studies in pediatric cohorts suggest cervicothoracic predominance.<sup>13,15</sup> Most prior studies report a predominantly longitudinally extensive myelitis (63%–93%) in MOGAD,<sup>14–17,20</sup> while Xu et al<sup>13</sup> report short segment involvement in 50%, similar to our findings. There are also mixed data on cross-sectional involvement of the cord, with our study demonstrating central cord involvement in slightly more than one-half of the cases and central gray matter involvement in 36%. The central gray matter involvement is described in pediatric MOGAD in ~50%.<sup>20,29</sup> These differences in previous reports might be due

**Table 3: Orbit and spine MR imaging features at presentation for serum antibody-positive MOGAD**

| Orbital Involvement                      | n = 31       | Spine Involvement        | n = 11      |
|--|--------------|--------------------------|-------------|
| Unilateral                               | 6/31 (19.4)  | Long segment             | 4/11 (36.4) |
| Bilateral                                | 25/31 (80.6) | Short segment            | 6/11 (54.5) |
| Segments involved                        |              | Cauda equina enhancement | 1/11 (9.1)  |
| Orbital                                  | 24/31 (77.4) | Focality                 |             |
| Intracanalicular                         | 20/31 (64.5) | Unifocal                 | 3/11 (27.3) |
| Prechiasmatic                            | 17/31 (54.8) | Multifocal               | 8/11 (72.7) |
| Optic chiasm                             | 5/31 (16.1)  | Location                 |             |
| Optic tract                              | 4/31 (12.9)  | Cervical                 | 8/11 (72.7) |
| Optic nerve enhancement <sup>a</sup>     | 25/29 (86.2) | Thoracic                 | 6/11 (54.5) |
| Perineural enhancement <sup>b</sup>      | 17/25 (68)   | Conus                    | 5/11 (45.4) |
| Optic nerve low diffusivity <sup>c</sup> | 10/15 (66.7) | Cauda equina             | 1/11 (9)    |
|  |              | Pattern                  |             |
|  |              | Central                  | 6/11 (54.5) |
|  |              | Peripheral               | 4/11 (36.4) |
|  |              | Entire cross-section     | 3/11 (27.3) |
|  |              | Central gray only        | 4/11 (36.4) |
|  |              | Enhancement              |             |
|  |              | None                     | 7/11 (63.6) |
|  |              | Intramedullary           | 3/11 (27.3) |
|  |              | Leptomeningeal           | 1/11 (9)    |
|  |              | Cord expansion           | 5/11 (45.4) |

<sup>a</sup>Unknown in 2 patients due to absence of contrast.

<sup>b</sup>Unknown in 6 patients due to absence of contrast and/or fat saturation.

<sup>c</sup>Unknown in 16 patients due to missing DWI sequence.

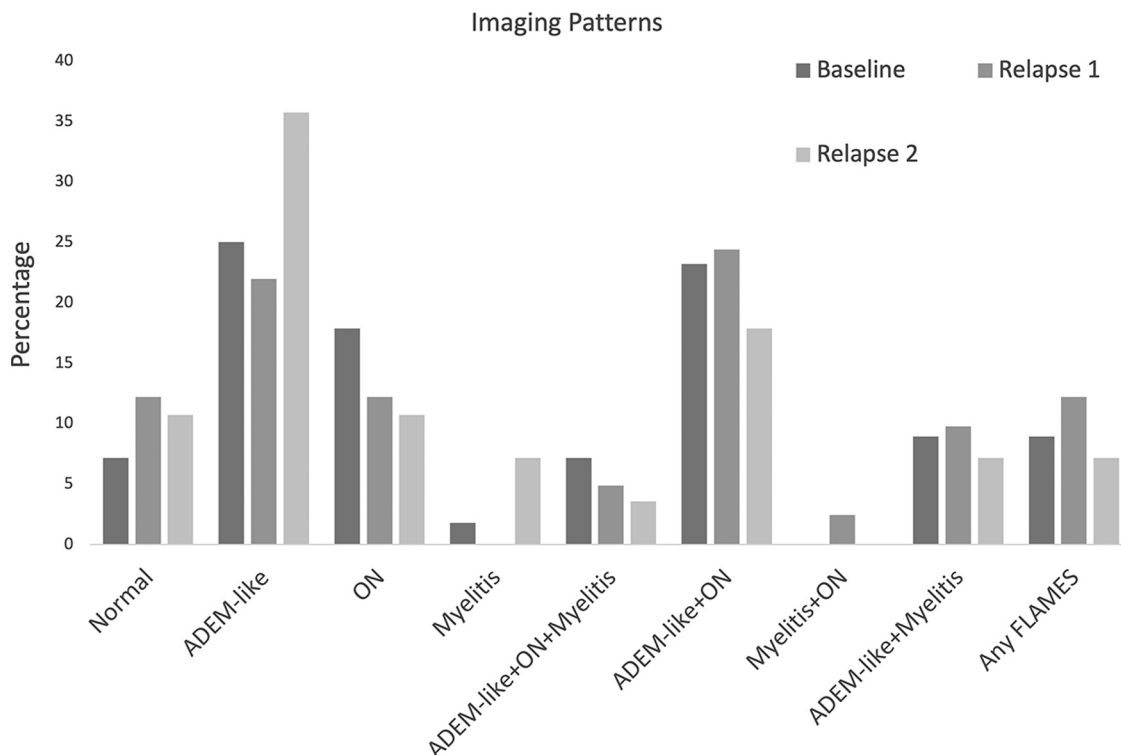


**FIG 3.** Imaging patterns at presentation and relapses.

**Table 4: Variation of imaging patterns at relapse stratified by age greater or less than 9 years**

|                              | Relapse 1          |                    |         | Relapse 2          |                    |         |
|------------------------------|--------------------|--------------------|---------|--------------------|--------------------|---------|
|                              | Age ≤9<br>(n = 23) | Age >9<br>(n = 18) | P Value | Age ≤9<br>(n = 13) | Age >9<br>(n = 15) | P Value |
| Normal                       | 1/23 (4.3)         | 4/18 (22.2)        | .008    | 1/13 (7.7)         | 2/15 (13.3)        | .211    |
| ADEM-like                    | 8/23 (34.8)        | 1/18 (5.6)         |         | 8/13 (61.5)        | 2/15 (13.3)        |         |
| ON                           | 3/23 (13.0)        | 2/18 (11.1)        |         | 1/13 (7.7)         | 2/15 (13.3)        |         |
| Myelitis                     |                    |                    |         | 0                  | 2/15 (13.3)        |         |
| ADEM-like + ON +<br>myelitis | 2/23 (8.7)         | 0                  |         | 0                  | 1/15 (6.7)         |         |
| ADEM-like + ON               | 7/23 (30.4)        | 3/18 (16.7)        |         | 2/13 (15.4)        | 3/15 (20)          |         |
| Myelitis + ON                | 0                  | 1/18 (5.6)         |         |                    |                    |         |
| ADEM-like + myelitis         | 2/23 (8.7)         | 2/18 (11.1)        |         | 1/13 (7.7)         | 1/15 (6.7)         |         |
| Any FLAMES                   | 0                  | 5/18 (27.8)        |         | 0                  | 2/15 (13.3)        |         |

to small sample size and relatively low prevalence of myelitis in pediatric MOGAD (45%–68%).<sup>15–17</sup>

Our findings are concordant with previous reports of age-related changes in imaging phenotype at presentation with predominantly ADEM-like presentation in younger children and ON in older children.<sup>2,5,10</sup> There are varying rates of relapse reported in pediatric MOGAD from 28% to 62%,<sup>4,7,9–11</sup> with our study on the higher end at 73.8%. This may partly be reflective of referral bias to our tertiary care center; however, this is an advantage of our study, as the higher relapse rates enable us to assess imaging and clinical factors associated with relapse. Clinical manifestations in relapsing pediatric MOGAD suggest varied phenotypes with some predominance of ON and myelitis<sup>7,9,23,30,31</sup> and change in phenotype between episodes in >50%.<sup>9</sup> There is limited published literature on imaging phenotypes at relapse, and our work adds to the literature in this respect. In our cohort, ON was present on imaging in 33%–45% at relapse and ADEM-like appearance on imaging in 60%–63%, which was more frequent at younger age of relapse. These age-dependent variations did not persist at second relapse, but this is difficult to interpret, given the small cohort of patients with second relapse and imaging.

There are mixed data on association of anti-MOG titer and risk of relapse.<sup>4,19</sup> We did not find an association between baseline anti-MOG titer and polyphasic disease. Previous reports indicate higher rate of recurrence among those with persistently high titers.<sup>4,9,31</sup> While older age has been associated with relapsing phenotype in prior studies,<sup>4,31</sup> in our study, older children had a shorter time to first relapse, which may be related to higher rates of persistent seropositivity in older children.<sup>31</sup>

Our study has several limitations. Given the retrospective study design, there is heterogeneity in available clinical, laboratory, and imaging data. The study included patients seen over 20 years, during which imaging techniques and MOGAD diagnosis and treatment have changed, further contributing to the data heterogeneity. All available MRIs corresponding to the first 3 clinical episodes were included in this study, including those performed at other institutions before referral and, hence, were of varying image quality and technique. However, only <2% were deemed to have poor subjective image quality by reviewers. Despite the relatively large sample size, the number of patients with spine involvement was low, limiting comprehensive

assessment of patterns of spine involvement. The use of immunosuppressants and disease-modifying therapy, which may affect the rate,<sup>5</sup> timing, and pattern of relapse, could not be adjusted for given variability in treatment, some of which occurred at other institutions.

## CONCLUSIONS

We describe the detailed imaging manifestations of pediatric MOGAD at presentation and at first 2 relapses. There are age-dependent variations in imaging phenotype at presentation and first relapse. Imaging phenotype at relapse

often differed from phenotype at presentation. Furthermore, older children tend to relapse sooner than younger children.

**Disclosure forms** provided by the authors are available with the full text and PDF of this article at [www.ajnr.org](http://www.ajnr.org).

## REFERENCES

- O'Connor KC, McLaughlin KA, De Jager PL, et al. **Self-antigen tetramers discriminate between myelin autoantibodies to native or denatured protein.** *Nat Med* 2007;13:211–17 [CrossRef Medline](#)
- Reindl M, Waters P. **Myelin oligodendrocyte glycoprotein antibodies in neurological disease.** *Nat Rev Neurol* 2019;15:89–102 [CrossRef Medline](#)
- de Mol CL, Wong YY, van Pelt ED, et al. **Incidence and outcome of acquired demyelinating syndromes in Dutch children: update of a nationwide and prospective study.** *J Neurol* 2018;265:1310–19 [CrossRef Medline](#)
- Hennes EM, Baumann M, Schanda K, BIOMARKER Study Group, et al. **Prognostic relevance of MOG antibodies in children with an acquired demyelinating syndrome.** *Neurology* 2017;89:900–08 [CrossRef Medline](#)
- Hacohen Y, Wong YY, Lechner C, et al. **Disease course and treatment responses in children with relapsing myelin oligodendrocyte glycoprotein antibody-associated disease.** *JAMA Neurol* 2018;75:478–87 [CrossRef Medline](#)
- Hacohen Y, Banwell B. **Treatment approaches for MOG-Ab-associated demyelination in children.** *Curr Treat Options Neurol* 2019;21:2 [CrossRef Medline](#)
- Lopez-Chiriboga AS, Majed M, Fryer J, et al. **Association of MOG-IgG serostatus with relapse after acute disseminated encephalomyelitis and proposed diagnostic criteria for MOG-IgG-associated disorders.** *JAMA Neurol* 2018;75:1355–63 [CrossRef Medline](#)
- Jarius S, Ruprecht K, Kleiter I, Neuromyelitis Optica Study Group (NEMOS), et al. **MOG-IgG in NMO and related disorders: a multicenter study of 50 patients. 1. Frequency, syndrome specificity, influence of disease activity, long-term course, association with AQP4-IgG, and origin.** *J Neuroinflammation* 2016;13:279 [CrossRef Medline](#)
- Armangue T, Olive-Cirera G, Martinez-Hernandez E, Spanish Pediatric anti-MOG Study Group, et al. **Associations of paediatric demyelinating and encephalitic syndromes with myelin oligodendrocyte glycoprotein antibodies: a multicentre observational study.** *Lancet Neurol* 2020;19:234–46 [CrossRef Medline](#)
- Fernandez-Carbonell C, Vargas-Lowy D, Musallam A, et al. **Clinical and MRI phenotype of children with MOG antibodies.** *Mult Scler* 2016;22:174–84 [CrossRef Medline](#)
- Wegener-Panzer A, Cleaveland R, Wendel EM, et al. **Clinical and imaging features of children with autoimmune encephalitis and**

- MOG antibodies.** *Neurol Neuroimmunol Neuroinflamm* 2020;7:e731 [CrossRef](#)
12. Hennes EM, Baumann M, Lechner C, et al. **MOG spectrum disorders and role of MOG-antibodies in clinical practice.** *Neuropediatrics* 2018;49:3–11 [CrossRef Medline](#)
  13. Xu J, Liu L, Xiong J, et al. **The clinical, radiologic, and prognostic differences between pediatric and adult patients with myelin oligodendrocyte glycoprotein antibody-associated encephalomyelitis.** *Front Neurol* 2021;12:679430 [CrossRef Medline](#)
  14. Baumann M, Bartels F, Finke C, E.U. Paediatric MOG Consortium, et al. **E.U. Paediatric MOG Consortium Consensus: 2. Neuroimaging features of paediatric myelin oligodendrocyte glycoprotein antibody-associated disorders.** *Eur J Paediatr Neurol* 2020;29:14–21 [CrossRef Medline](#)
  15. Baumann M, Grams A, Djurdjevic T, et al. **MRI of the first event in pediatric acquired demyelinating syndromes with antibodies to myelin oligodendrocyte glycoprotein.** *J Neurol* 2018;265:845–55 [CrossRef Medline](#)
  16. Baumann M, Sahin K, Lechner C, et al. **Clinical and neuroradiological differences of paediatric acute disseminating encephalomyelitis with and without antibodies to the myelin oligodendrocyte glycoprotein.** *J Neurol Neurosurg Psychiatry* 2015;86:265–72 [CrossRef Medline](#)
  17. Konuskan B, Yildirim M, Gocmen R, et al. **Retrospective analysis of children with myelin oligodendrocyte glycoprotein antibody-related disorders.** *Mult Scler Relat Disord* 2018;26:1–7 [CrossRef Medline](#)
  18. Banwell B, Bennett JL, Marignier R, et al. **Diagnosis of myelin oligodendrocyte glycoprotein antibody-associated disease: International MOGAD Panel proposed criteria.** *Lancet Neurol* 2023;22:268–82 [CrossRef Medline](#)
  19. Lui A, Chong J, Flanagan E, et al. **High titers of myelin oligodendrocyte glycoprotein antibody are only observed close to clinical events in pediatrics.** *Mult Scler Relat Disord* 2021;56:103253 [CrossRef Medline](#)
  20. Tantsis EM, Prelog K, Alper G, Paediatric Myelitis MRI Study Group, et al. **Magnetic resonance imaging in enterovirus-71, myelin oligodendrocyte glycoprotein antibody, aquaporin-4 antibody, and multiple sclerosis-associated myelitis in children.** *Dev Med Child Neurol* 2019;61:1108–16 [CrossRef Medline](#)
  21. Salama S, Khan M, Levy M, et al. **Radiological characteristics of myelin oligodendrocyte glycoprotein antibody disease.** *Mult Scler Relat Disord* 2019;29:15–22 [CrossRef Medline](#)
  22. Dubey D, Pittock SJ, Krecke KN, et al. **Clinical, radiologic, and prognostic features of myelitis associated with myelin oligodendrocyte glycoprotein autoantibody.** *JAMA Neurol* 2019;76:301–09 [CrossRef Medline](#)
  23. Cobo-Calvo A, Ruiz A, D'Indy H, et al. **MOG antibody-related disorders: common features and uncommon presentations.** *J Neurol* 2017;264:1945–55 [CrossRef Medline](#)
  24. Garbugio Dutra B, da Rocha AJ, Hoffmann Nunes R, et al. **Neuromyelitis optica spectrum disorders: spectrum of MR imaging findings and their differential diagnosis.** *Radiographics* 2018;38:169–193 [CrossRef Medline](#)
  25. Song H, Zhou H, Yang M, et al. **Clinical characteristics and outcomes of myelin oligodendrocyte glycoprotein antibody-seropositive optic neuritis in varying age groups: a cohort study in China.** *J Neurol Sci* 2019;400:83–89 [CrossRef Medline](#)
  26. Wendel EM, Baumann M, Barisic N, et al. **High association of MOG-IgG antibodies in children with bilateral optic neuritis.** *Eur J Paediatr Neurol* 2020;27:86–93 [CrossRef Medline](#)
  27. Sato DK, Callegaro D, Lana-Peixoto MA, et al. **Distinction between MOG antibody-positive and AQP4 antibody-positive NMO spectrum disorders.** *Neurology* 2014;82:474–81 [CrossRef Medline](#)
  28. Kitley J, Waters P, Woodhall M, et al. **Neuromyelitis optica spectrum disorders with aquaporin-4 and myelin-oligodendrocyte glycoprotein antibodies: a comparative study.** *JAMA Neurol* 2014;71:276–83 [CrossRef Medline](#)
  29. Wang C, Narayan R, Greenberg B. **Anti-myelin oligodendrocyte glycoprotein antibody associated with gray matter predominant transverse myelitis mimicking acute flaccid myelitis: a presentation of two cases.** *Pediatr Neurol* 2018;86:42–45 [CrossRef Medline](#)
  30. Ramanathan S, Mohammad S, Tantsis E, Australasian and New Zealand MOG Study Group, et al. **Clinical course, therapeutic responses and outcomes in relapsing MOG antibody-associated demyelination.** *J Neurol Neurosurg Psychiatry* 2018;89:127–37 [CrossRef Medline](#)
  31. Waters P, Fadda G, Woodhall M, Canadian Pediatric Demyelinating Disease Network, et al. **Serial anti-myelin oligodendrocyte glycoprotein antibody analyses and outcomes in children with demyelinating syndromes.** *JAMA Neurol* 2020;77:82–93 [CrossRef Medline](#)